17. J. Alroy *et al.*, *Proc. Natl. Acad. Sci. U.S.A.* **98**, 6261 (2001).
18. R. K. Bambach, A. H. Knoll, J. J. Sepkoski, *Proc. Natl. Acad. Sci. U.S.A.* **99**, 6854 (2002).
19. A. K. Behrensmeyer *et al.*, *Paleobiology* **31**, 607 (2005).
20. J. R. Pawlik, *Chem. Rev.* **93**, 1911 (1993).
21. J. J. Sepkoski, *Bull. Am. Paleo.* **363**, 1 (2002).
22. M. A. Buzas, C. F. Koch, S. J. Culver, N. F. Sohl, *Paleobiology* **8**, 143 (1982).
23. E. S. Vrba, S. J. Gould, *Paleobiology* **12**, 217 (1986).
24. We thank D. Bottjer, S. Holland, L. Ivany, A. Miller, and M. Patzkowsky for helpful discussions, and M. Apel, N. Bonuso, P. Borkow, B. Brenneis, M. Clapham, L. Fall, C. Ferguson, M. Foote, M. Gibson, T. Hanson, N. Heim, D. Hempfling, A. Hendy, S. Hicks, S. Holland, C. Jamet, K. Koverman, Z. Krug, K. Layou, E. Leckey, A. McGowan, P. Novack-Gottshall, S. Nürnberg, J. Sessa, C. Simpson, A. Tomasovych, and P. Wall for data collection. B. Kroeger and D. Korn helped to categorize the life habits of the Cephalopoda. This work was conducted at the National Center for Ecological Analysis and Synthesis, a center funded by NSF grant DEB-0072909, the University of California, and the University of California at Santa Barbara. This is Paleobiology Database publication number 44.

Supporting Online Material
www.sciencemag.org/cgi/content/full/312/5775/897/DC1
Materials and Methods
Table S1
References

8 December 2005; accepted 24 March 2006
10.1126/science.1123591

Fall in Earth's Magnetic Field Is Erratic

David Gubbins,* Adrian L. Jones, Christopher C. Finlay†

Earth's magnetic field has decayed by about 5% per century since measurements began in 1840. Directional measurements predate those of intensity by more than 250 years, and we combined the global model of directions with paleomagnetic intensity measurements to estimate the fall in strength for this earlier period (1590 to 1840 A.D.). We found that magnetic field strength was nearly constant throughout this time, in contrast to the later period. Extrapolating to the core surface showed that the fall in strength originated in patches of reverse magnetic flux in the Southern Hemisphere. These patches were detectable by directional data alone; the pre-1840 model showed little or no evidence of them, supporting the conclusion of a steady dipole up to 1840.

Jackson *et al.*'s historical model of the geomagnetic field (*1*) covers the period 1590 A.D. to the present (Fig. 1). Measurements of direction (declination and inclination) are available throughout this period, although inclination is scarce in the 17th century. No absolute intensity data are available until 1837, when C. F. Gauss devised the first method to measure it; intensity measurements became widespread by 1840. The EarthRef Digital Archive (ERDA) has an internally consistent paleointensity database compiled by Korte *et al.* (*2*). It contains 315 measurements on rock samples and archaeological remains from the interval 1590 to 1840 A.D., and we can, in principle, use these to determine field strength during the early period when there were no direct measurements.

The paleointensity data have error estimates on both intensity and age. Dating errors vary from 1 year, when historical records date the specimen precisely, to centuries, when only radiocarbon dates are available. Geographical coverage is poor (Fig. 2), with concentration in Europe and very little representation in the Southern Hemisphere, but temporal coverage is good (Fig. 3). Intensities have typical errors of 4000 nT, or about 10%. This error is comparable with any change expected during the entire period, so paleointensity measurements provide no usable information on intensity variation at a single site. However, given good directional information from the historical model, each intensity measurement can be converted to an estimate of the dipole moment, or g_1^0 (t), because a theorem (*3*) states that, given perfect directional information and no more than two dip-poles (places where the magnetic field is vertical, of which the Earth has only two), a single intensity measurement determines the field uniquely. The poor geographical coverage of intensity is therefore largely irrelevant, provided the global coverage of direction is good. Here we assume that g_1^0 (t) fell linearly from 1590 to 1840 and fix its value at 1840 to be that of the historical field model. This leaves just one parameter, the slope of the line, to be determined from 315 measurements. This large number of data are able to produce a meaningful estimate of a single unknown, the slope, despite the large errors on an individual datum.

We use the iterative maximum likelihood method of Williamson (*4*), closely related to that described by Press *et al.* (*5*), to fit a straight line through data having errors in both magnitude and time. g_1^0 (t = 1840) is constrained by

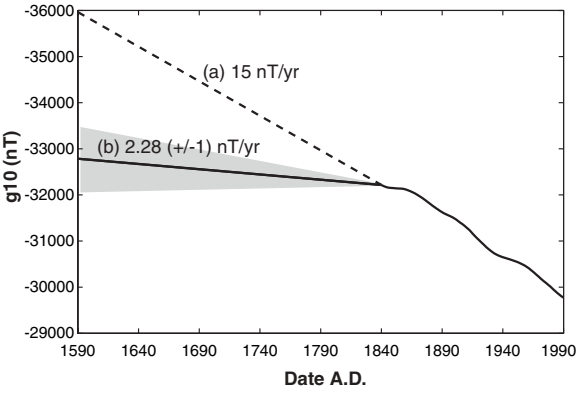

Fig. 1. Fall of the geomagnetic coefficient g_1^0 (in nT) since measurements began in 1590. g_1^0 is proportional to the Earth's dipole moment. Intensity measurements became available in 1840; the two slopes before 1840 are (a) the extrapolation back in time based on the average fall since 1840 and (b) paleointensity measurements using the method described in the present study. Shaded area gives the ±1 SD slopes.

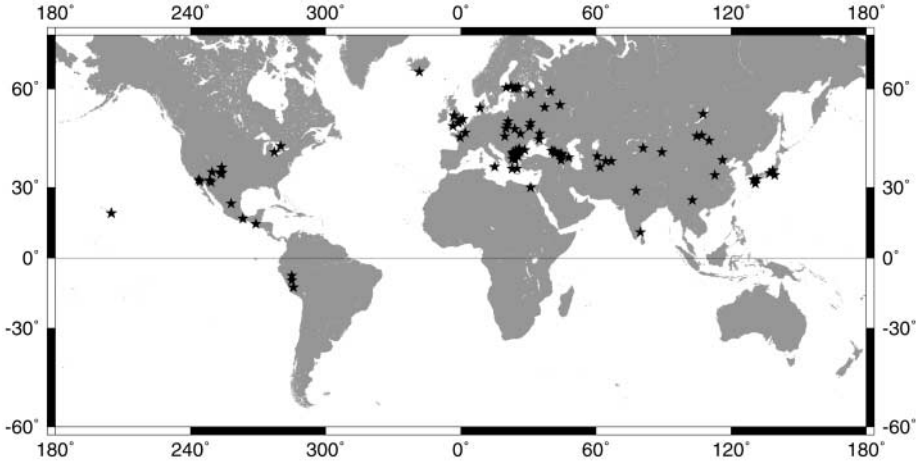

Fig. 2. Geographical distribution of the paleointensity data from 1590 to 1840 A.D. Data are mostly from the Northern Hemisphere, but the Southern Hemisphere is well covered by directional measurements.

School of Earth and Environment, University of Leeds, Leeds LS2 9JT, UK.

*To whom correspondence should be addressed. E-mail: gubbins@earth.leeds.ac.uk
†Present address: Institut für Geophysik, ETH Zürich, Switzerland.

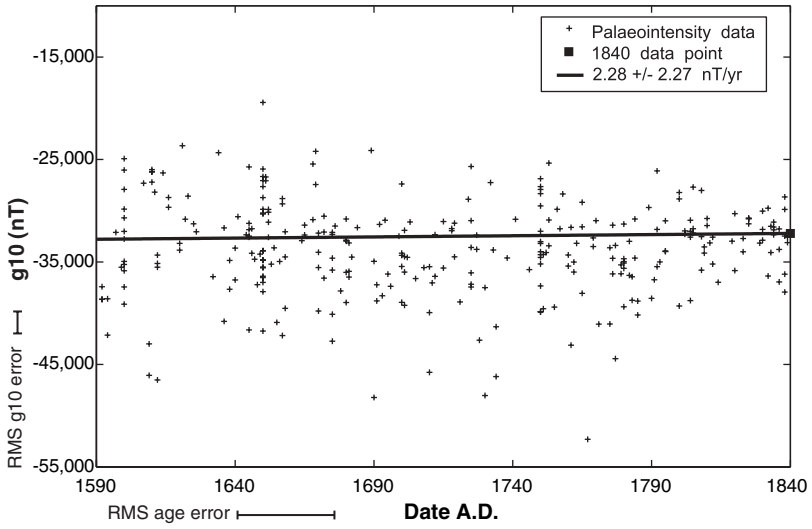

Fig. 3. Paleointensity data converted to g_1^0. The line is tied to the value at 1840 (black square), which is accurately determined by historical measurements. Root mean square (RMS) g_1^0 and age errors are shown as bars along the axes; they are 1943 nT and 35 years, respectively.

adding a single data point with very high accuracy. The method produces an estimate of the slope, its standard deviation, and a χ^2 goodness-of-fit parameter; it requires the data errors to be independent and normally distributed, which we confirmed by plotting histograms. The fit produced a slope of $\dot{g}_1^0 = 2.28 \pm 2.72$ nT/year (Fig. 1) and $\chi^2 = 258$. This value of χ^2, with 314 degrees of freedom, indicates a good fit; the probability of $\chi^2 \leq 258$ occurring by chance is 0.99. We conclude that a straight line fits the data well and a more complicated curve is not justified. A Student's t test indicates that the derived slope of 2.28 nT/year differs significantly from the post-1840 average of 15 nT/year with better than 99.999% confidence. This result is vulnerable to small systematic errors in the paleointensity data; they would need to be systematically slightly low in early times to account for the small slope. We find no reason for such a systematic error nor any systematic correlation with experimental procedure, author, or geographical site. Our result

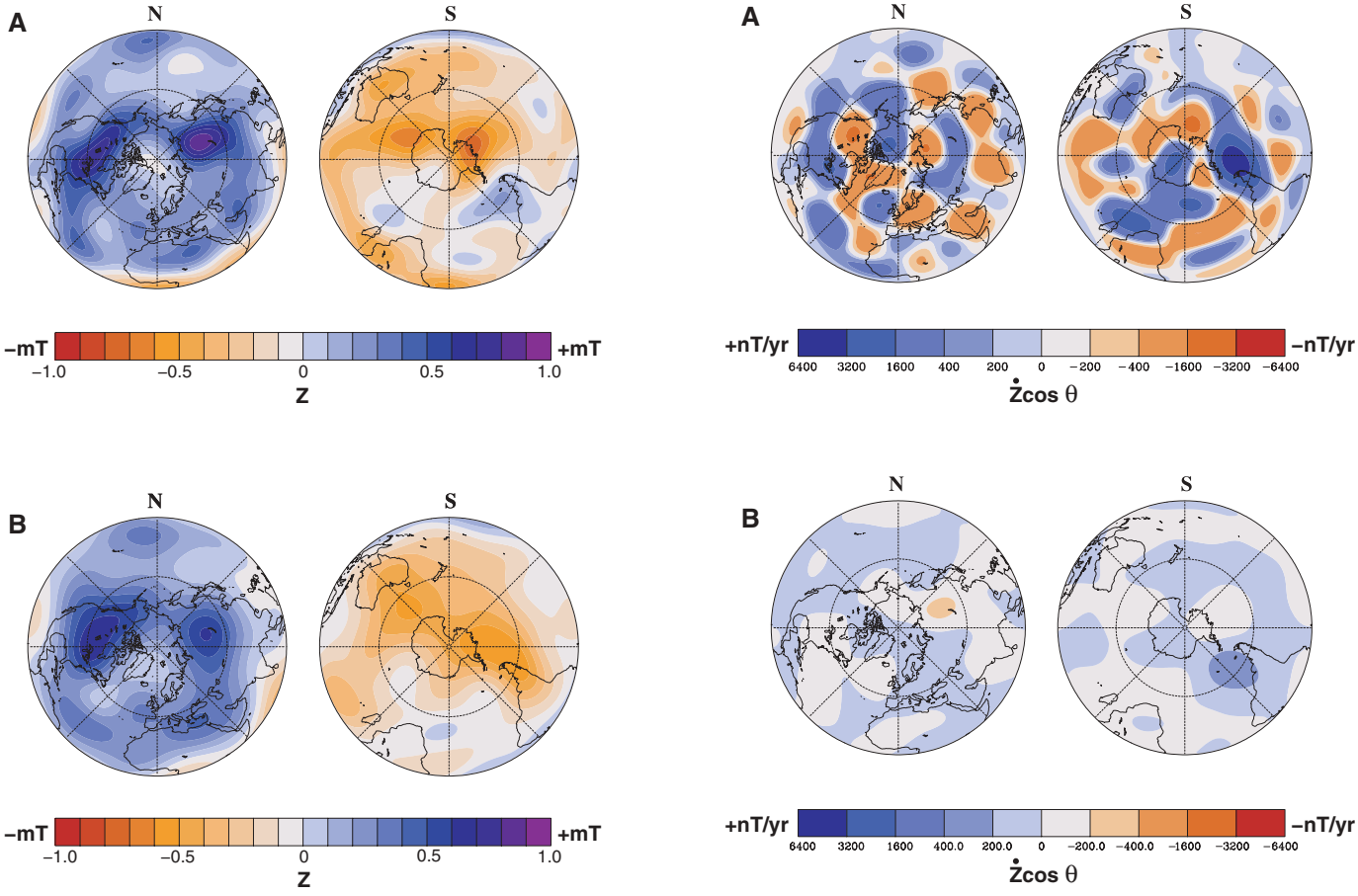

Fig. 4. (**left**). Vertical component of magnetic field Z on the core-mantle boundary in Lambert equal-area projection averaged over the interval 1840 to 1980 (**A**) and 1590 to 1840 (**B**). The general dipolar structure is reflected in the dominance of blue (inward flux) in the Northern Hemisphere (left) and orange (outward flux) in the Southern Hemisphere (right). Reverse-flux patches show up as blue in the Southern Hemisphere in 1980; these have been growing and moving south in recent decades and are the major contributor to the present fall in dipole moment. They are largely absent from the 1780 map and are not seen in earlier times. **Fig. 5.** (**right**). Contributions to the changing dipole moment over the interval 1840 to 1980 (**A**) and 1590 to 1840 (**B**). Shown is $\dot{Z}\cos\theta$, where $\dot{Z}$ is the secular variation of the vertical component of magnetic field at the core-mantle boundary and θ is the colatitude, in Lambert equal-area projection, averaged over each time interval. The fall in dipole moment over the period is given by the integral over both hemispheres (Eq. 1). The predominance of blue in the Southern Hemisphere from 1840 to 1980 [(A), right], associated with the growth and southward movement of reverse-flux patches, is responsible for almost all of the fall in dipole moment during this period.

is consistent with Korte and Constable's low-resolution geomagnetic field model CALS7K.2 (*6*, *7*), which has a slower decay of the dipole moment from 1600 to 1800 A.D. compared with that from 1800 to 1950 A.D. Their model, which spans the interval 5000 B.C. to 1950 A.D., was constructed from paleointensity and paleodirection data only (*2*, *6*) and therefore lacks information from the vastly more accurate historical measurements included in the present study.

What changed to precipitate the present fall in dipole moment? More insight comes from directional data, which are excellent from 1700 A.D. and suggest a change occurring around 1800 A.D. The geomagnetic field originates in the liquid core, and its dipole moment may be written as an average of the magnetic field at the core surface

$$g_1^0 = \frac{3c}{8\pi a^3}\int_S Z\cos\theta dS \qquad (1)$$

where Z is the downward component of magnetic field; θ is colatitude; a and c are Earth and core radii, respectively; and the integral is taken over the surface S of the liquid core. The source of any change in dipole moment can therefore be found from the change in $Z\cos\theta$ on the core surface, which comes mostly from growth and southward migration of patches of reversed flux in the Southern Hemisphere (Fig. 4). No intensity information is required to identify these reverse-flux patches; they are imaged well by the early directional data. One distinct patch first appeared in about 1780 A.D. (*8*) and continues to grow and drift south today (*8*, *9*).

An equal-area plot of $\dot{Z}\cos\theta$ reveals the regions on the core surface responsible for the fall (Fig. 5). The interval 1840 to 1980 (Fig. 5A) is dominated by the blue patch between Antarctica and the tip of South America, with additional contributions from other blue patches in the Southern Hemisphere. Orange and blue patches in the Northern Hemisphere are of similar size and cancel out. The separate contributions of the two hemispheres to the change in g_1^0 is $(\dot{g}_N, \dot{g}_S, \dot{g}_1^0) = (-0.1, 16.2, 16.1)$ nT/year, showing that almost all of the dipole decay has come from the Southern Hemisphere.

The interval 1590 to 1840 A.D. (Fig. 5B), which uses the mean fall in g_1^0 of 2.28 nT/year obtained in this study, shows much smaller amplitudes, and the patch between Antarctica and South America is almost balanced by the patches of opposite sign to the west, indicating longitudinal drift rather than southward movement or growth. The separate contributions of the integral for this interval are $(\dot{g}_N, \dot{g}_S, \dot{g}_1^0) = (-0.8, 3.1, 2.3)$; the Northern Hemisphere value is again effectively zero, but the Southern Hemisphere value is much lower than in the 19th and 20th centuries. This is consistent with a change in Southern Hemisphere behavior starting around 1800 A.D.; before that date the two hemispheres behaved in a similar manner.

Paleomagnetic data from the past 2500 years suggest a 40% fall in moment (*6*, *10*), or 1.6% per century. This is smaller than the present fall (5% per century) and is consistent with periods of rapid fall, as at present, interspersed with periods of little or no activity, as during 1590 to 1840 A.D. Patches of reverse flux almost certainly arise from expulsion of toroidal flux (*11*), and our present result suggests a quiet period up to 1800 when toroidal flux was brought up close to the core surface followed by active periods of expulsion through the core surface. The challenge now is to understand the magnetohydrodynamics of how such behavior can come about and to discover similar, earlier intervals of dipole decay interspersed with quiescence in the paleomagnetic record.

References and Notes

1. A. Jackson, A. R. T. Jonkers, M. R. Walker, *Philos. Trans. R. Soc. London A* **358**, 957 (2000).
2. M. Korte, A. Genevey, C. G. Constable, U. Frank, E. Schnepp, *Geochem. Geophys. Geosyst.* 10.1029/2004GC000800 (1 February 2005).
3. G. Hulot, A. Khokhlov, J. L. LeMouel, *Geophys. J. Int.* **129**, 347 (1997).
4. J. H. Williamson, *Can. J. Phys.* **46**, 1846 (1968).
5. W. H. Press, B. P. Flannery, S. A. Teukolsky, W. T. Vetterling, *Numerical Recipes in FORTRAN* (Cambridge Univ. Press, Cambridge, UK, 2002).
6. M. Korte, C. G. Constable, *Geochem. Geophys. Geosyst.* 10.1029/2004GC000801 (1 February 2005).
7. M. Korte, C. G. Constable, *Earth Planet. Sci. Lett.* **236**, 348 (2005).
8. J. Bloxham, D. Gubbins, A. Jackson, *Philos. Trans. R. Soc. London* **329**, 415 (1989).
9. G. Hulot, C. Eymin, B. Langlais, M. Mandea, N. Olsen, *Nature* **416**, 620 (2002).
10. M. W. McElhinny, W. E. Senanayake, *J. Geomagn. Geoelectr.* **34**, 39 (1980).
11. D. Gubbins, *Phys. Earth Planet. Int.* **98**, 193 (1996).

12. This work formed part of A.L.J.'s undergraduate project, which was supported by a Local Education Authority grant. C.C.F. was supported by a Ph.D. studentship from the Natural Environment Research Council (NER/S/A/2001/06265).

11 January 2006; accepted 14 March 2006
10.1126/science.1124855

Impaired Control of IRES-Mediated Translation in X-Linked Dyskeratosis Congenita

Andrew Yoon,[1]* Guang Peng,[1]* Yves Brandenburg,[1]* Ornella Zollo,[1] Wei Xu,[1] Eduardo Rego,[2] Davide Ruggero[1]†

The *DKC1* gene encodes a pseudouridine synthase that modifies ribosomal RNA (rRNA). *DKC1* is mutated in people with X-linked dyskeratosis congenita (X-DC), a disease characterized by bone marrow failure, skin abnormalities, and increased susceptibility to cancer. How alterations in ribosome modification might lead to cancer and other features of the disease remains unknown. Using an unbiased proteomics strategy, we discovered a specific defect in IRES (internal ribosome entry site)–dependent translation in *Dkc1*^{m} mice and in cells from X-DC patients. This defect results in impaired translation of messenger RNAs containing IRES elements, including those encoding the tumor suppressor p27(Kip1) and the antiapoptotic factors Bcl-xL and XIAP (X-linked Inhibitor of Apoptosis Protein). Moreover, *Dkc1*^{m} ribosomes were unable to direct translation from IRES elements present in viral messenger RNAs. These findings reveal a potential mechanism by which defective ribosome activity leads to disease and cancer.

X-linked dyskeratosis congenita (X-DC) is a rare and often fatal disease characterized by multiple pathological features, including bone marrow failure and increased susceptibility to cancer (*1*). X-DC is caused by mutations in the *DKC1* gene that encodes dyskerin, a protein associated with small RNAs that share the H+ACA RNA motif, including the telomerase RNA (TR), Cajal body RNAs (scaRNAs), and small nucleolar RNAs (snoRNAs) (*2*). When associated with snoRNAs, dyskerin acts as a pseudouridine synthase to mediate posttranscriptional modification of ribosomal RNA (rRNA) through the conversion of uridine (U) to pseudouridine (Ψ) (*3*, *4*). X-DC patient cell lines and mouse embryonic stem cells harboring knocked-in *DKC1* point mutations exhibit reduced rRNA pseudouridylation (*2*, *5*). Hypomorphic *Dkc1*^{m} mice recapitulate many of the clinical features of X-DC and display reductions in rRNA modification, suggesting that impairments in ribosome function may have a causative effect on X-DC pathogenesis (*6*). However, the role of rRNA modifications in the control of protein synthesis remains poorly understood. In addition, how alterations in the translational apparatus could lead to specific pathological features associated with human disease remains unknown. We investigated the role of rRNA modifications in the control of protein synthesis in order to understand the molecular basis of X-DC.

[1]Human Genetics Program, Fox Chase Cancer Center, Philadelphia, PA 19111, USA. [2]Center for Cell Based Therapy, Fundação Hemocentro de Ribeirão Preto, University of Sao Paulo, Brazil.

*These authors contributed equally to this work.
†To whom correspondence should be addressed. E-mail: davide.ruggero@fccc.edu